CALCULATION OF THE DISCHARGE OF UNDERGROUND EXPLOSION GASES INTO THE ATMOSPHERE

V. V. Adushkin and P. B. Kaazik

UDC 550.348.42

Nonstationary gas filtration from the cavity of a camouflaged underground explosion through a disaggregated porous medium is calculated. The computations were carried out for a spherically symmetric gas experiencing two-dimensional motion. A two-term law of filtration was used. The space–time pressure distribution of the gas within the medium was obtained. Motion hodographs of the "front" of filtration and the interface between the explosion products and air were constructed. The influence of the soil filtration characteristics and pressure in the cavity was investigated. The time at which gas is discharged into the atmosphere is determined based on well-known data on the permeability of certain types of rocks that have undergone the effects of an explosion. The variation of gas flow with time as a function of explosion depth is established.

Underground camouflaged explosions are characterized by an insignificant rise in the free soil surface. Nevertheless, in the overwhelming majority of such exposions the soil mass is in the disaggregated state right up to the crestal plane as a result of the effect of compression and dilation waves and also due to preferred upwards displacement. A process in which explosion gases appear in the many cracks and pores of the surrounding mass and their subsequent extrusion into the atmosphere therefore occurs at the final stage of camouflaged explosions due to the effect of excess pressure in the cavity. Concepts from filtration theory [1-3] can be used to describe such gas motion. A similar mechanism for the discharge of explosion gases is typical for sufficiently sturdy rock, in which the cavity either does not cave in or does cave in at a sufficiently later point in time.

A theoretically distinct mechanism for the discharge of gases into the atmosphere due to continuous caving in of the cavity up to the crestal plane is possible in loose ground. Some results of measurement of the time at which gas is discharged into the atmosphere according to this mechanism have been set forth in [4] in the case of an ideally free-flowing medium. A combination of both gas-discharge mechanisms is possible under actual conditions of carrying out underground explosions, depending on the scale of the explosion and the geological structure of the massif.

In the current work, the problem will be formulated in the following way. A cavity of finite radius r_0 with cavity gas pressure p_1 exists in a disaggregated permeable medium at the initial moment of time. Gas filters from the cavity under the effect of pressure. The pores and cracks of the medium are filled with air at an initial pressure p_0. We have assumed in solving the problem that: 1) the disaggregated medium has ceased moving; 2) medium porosity in the course of gas motion remains invariant; 3) gas motion through the disaggregated medium is descibed by a filtration equation that contains linear and quadratic terms; 4) gas–medium heat exchange is not taken into account; and 5) cavity gas and air in the pores are assumed to have identical constant viscosity.

We note that the results of a solution of this problem can also be useful in studying the process by which the stressed state of a solid medium breaks down and varies due to gas from an explosion penetrating the cracks.

The nonsteady motion of a filtering gas is described in the one-dimensional case using Euler variables by the mass preservation law

Moscow. Translated from Zhurnal Prikladnoi Mekhaniki i Tekhnicheskoi Fiziki, No. 1, pp. 111-120, January-February, 1976. Original article submitted November 27, 1974.

$$\frac{\partial \rho}{dt} = \frac{1}{m}\left[\frac{\partial}{\partial r}(\rho q) + \frac{(\nu-1)}{r}\rho q\right] \tag{1}$$

and a two-term Darcy law

$$-\frac{\partial p}{\partial r} = \frac{\mu}{k} q + \frac{\rho q^2}{k_t} \operatorname{sgn} q, \tag{2}$$

where p is pressure, ρ is density, μ is gas viscosity, q is filtration rate, m is porosity, k and k_t are the permeabilities in laminar and turbulent flow of the filtering gas, and ν is the dimension of the problem (ν = 1 in two-dimensional and $\nu = 3$ in spherically symmetric gas motion).

The equation of state of the filtering gas is taken in the form

$$\rho = Ap^n. \tag{3}$$

We assume that the mass formed as the gas explodes remains invariant during the filtration process, and that the condition on the cavity boundary is described by the equation

$$\frac{\partial \rho_c}{\partial t} = -(\rho_c q)\frac{S}{V},$$

where $\rho_c = Bp^{n_1}c$ is the equation of state of the gas in the cavity and S and V are cavity surface and volume, respectively.

It is natural to specify the pressure distribution at the initial moment of time in the form

$$p(r, 0) = \begin{cases} p_1 \text{ when } r = r_0, \\ p_0 \text{ when } r > r_0. \end{cases} \tag{4}$$

We eliminate ρ and q from Eqs. (1)-(3), obtaining a single nonlinear second-order partial differential equation in p,

$$\frac{\partial p^n}{\partial t} = \frac{k}{m\mu}\left[\frac{\partial}{\partial r}\left(p^n \frac{\partial p}{\partial r}\right)\frac{1}{G} + \frac{\nu-1}{r}\frac{\mu^2 k_t}{2k^2\delta A}(G-1)\right], \tag{5}$$

with the boundary condition at $r = r_0$

$$\frac{\partial p^{n_1}}{\partial t} = \frac{S}{V}\frac{\mu k_t}{2Bk\delta}(G_1 - 1), \tag{6}$$

where

$$\delta = -\operatorname{sgn} q = \operatorname{sgn}\frac{\partial p}{\partial r};\quad G = \sqrt{1 + 4\frac{k^2 A\delta}{\mu^2 k_t} p^n \frac{\partial p}{\partial r}}.$$

Equations (5) and (6) imply that the solution has the form

$$p = f\left(p_0; p_1; r_0; n; n_1; \frac{k}{\mu m}; \frac{Ak^2}{\mu^2 k_t}; \frac{S\mu k_t}{VBk}; t; r\right). \tag{7}$$

We introduce the dimensionless parameters

$$H = p/p_1;\ H_0 = p_0/p_1;\ \alpha = \frac{Ak^2 p_1^{n+1}}{\mu^2 k_t r_0};$$
$$\beta = \frac{Sr_0 mA}{VBp_1^{n_1-n}};\ \tau = \frac{kp_1 t}{m\mu r_0^2};\ x = r/r_0,$$

so that Eq. (7) is written in the form

$$H = f(H_0; n; n_1; \alpha; \beta; x; \tau). \tag{8}$$

As a result, Eq. (5) in dimensionless form convenient for programming takes the form

$$\frac{\partial H^n}{\partial \tau} = \frac{1}{G}\frac{\partial}{\partial x}\left(H^n \frac{\partial H}{\partial x}\right) + \frac{\nu-1}{x}\frac{2H^n \frac{\partial H}{\partial x}}{(G+1)};\quad G = \sqrt{1 + 4\alpha H^n \left|\frac{\partial H}{\partial x}\right|} \tag{9}$$

under the boundary and initial conditions

$$\frac{\partial H^{n_1}}{\partial \tau} = \frac{2\beta}{G_1 + 1} H^{n_1}\frac{\partial H}{\partial x};\quad G_1 = \sqrt{1 + 4\alpha H^{n_1}\left|\frac{\partial H}{\partial x}\right|} \text{ when } x = 1; \tag{10}$$

$$H(1,\ 0)=1;\ H(x,\ 0)=H_0 \text{ when } \tau=0, \tag{11}$$

and we require that all the functions be bounded as $x\to\infty$.

Thus, the problem has reduced to the solution of Eq. (9) under the boundary and initial conditions (10) and (11).

It is convenient to introduce the new function

$$Z(x,\tau)=\begin{cases}[H(x,\tau)]^{n_1} \text{ when } x=1,\\ [H(x,\tau)]^{n} \text{ when } x>1.\end{cases}$$

and pass to the finite-difference analog of the problem (9)-(11). We may write, using the Crank–Nicholson six-point method [5] with uniform grid and pitches h in coordinate x and $\Delta\tau$ in coordinate τ, the equations

$$\frac{Z(i,\ j+1)}{H(i,\ j+1)}-\frac{Z(i,\ j)}{H(i,\ j)}=\gamma\frac{\Delta\tau}{h^2(n+1)}\left\{\frac{1}{\sigma(i,\ j+1)}[Z(i+1,\ j+1)\right.$$
$$-2Z(i,\ j+1)+Z(i+1,\ j+1)]+\frac{(\nu-1)h}{x(i)[\sigma(i,\ j+1)+1]}[Z(i+1,\ j+1)$$
$$\left.-Z(i-1,\ j+1)]\right\}+(1+\gamma)\frac{\Delta\tau}{h^2(n+1)}\left\{\frac{1}{\sigma(i,\ j)}[Z(i+1,\ j)-2Z(i,j)\right.$$
$$\left.+Z(i-1,\ j)]+\frac{(\nu-1)h}{x(i)[\sigma(i,\ j)+1]}[Z(i+1,\ j)-Z(i-1,\ j)]\right\}; \tag{12}$$
$$\sigma(i,\ j)=\sqrt{1+\frac{2\alpha}{(n+1)h}|Z(i+1,\ j)-Z(i-1,\ j)|};$$
$$\frac{Z(0,\ j+1)}{H(0,\ j+1)}-\frac{Z(0,\ j)}{H(0,\ j)}=\gamma\frac{2\beta\Delta\tau}{(n_1+1)h[\sigma(0,\ j+1)]}$$
$$\times[Z(1,\ j+1)-Z(0,\ j+1)]+(1-\gamma)\frac{2\beta\Delta\tau}{(n_1+1)h[(\sigma,0,\ j+1)]}[Z(1,\ j)-Z(0,\ j)]; \tag{13}$$
$$\sigma(0,\ j)=\sqrt{1+\frac{4\alpha}{(n_1+1)h}|Z(1,\ j)-Z(0,\ j)|}\ .$$

Since the number of computation points is bounded, linear extrapolation to infinity is used at the right computation boundary,

$$Z(N-2,\ j)-2Z(N-1,\ j)+Z(N,\ j)=0. \tag{14}$$

The system of equations (12)-(14) consists of (N+1) equations with (N+1) unknowns, where N is the number of computation points in a single time stratum. The parameter γ may take values from zero to one, $\gamma=0$ resulting in an explicit four-point scheme, and $\gamma=1$, an implicit scheme. Practical computations have demonstrated that the best (from the point of view of computation accuracy and stability) is $\gamma\sim0.55$.

Equations (12)-(14) can be rewritten in the form

$$a(i-1)Z(i-1,\ j+1)-b(i)Z(i,\ j+1)+c(i+1)Z(i+1,\ j+1)$$
$$=-f(i,\ j),\ a(-1)=c(N+1)=0,\ i=0,\ \ldots,\ N. \tag{15}$$

The system (15) was solved using the factorization method [5]. In the course of the solution we first set H(i, j+1) = h(i, j), σ(i, j+1) = σ(i, j), and the values of H(i, j+1) and σ(i, j+1) were refined in terms of the resulting values of Z(i, j+1) until the error in Z was less than 0.001%. Actual experience demonstrated that two to three iterations were sufficient.

It is evident from Eqs. (12) and (13) that the discontinuity in the initial conditions (11) is eliminated by "spreading" by one step, i.e., taking H(0, 0) = 1 and H(h, 0) = H_0.

The program provides for the calculation of the dimensionless gas flow and the position of the interface between the cavity and interstitial gases $l(\tau)$. Computation precision is controlled by checking the mass balance over the entire space of compuation points.

The distinctive feature of the program is that the boundary of the computation region is variable. This was done on the basis of the analogy of our problem to heat-conductivity problems. It is well known that a linear heat-conductivity equation with initial conditions of the type of (4) and infinite right boundary has the solution of a propagating "thermal wave." Though the thermal wave instantaneously propagates to infinity, in practice a region may be indicated in which the temperature is identical to the initial temperature. Such

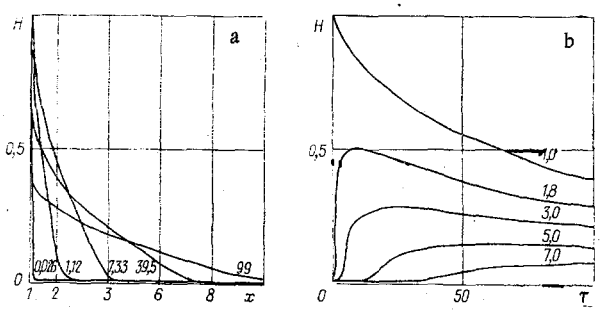

Fig. 1

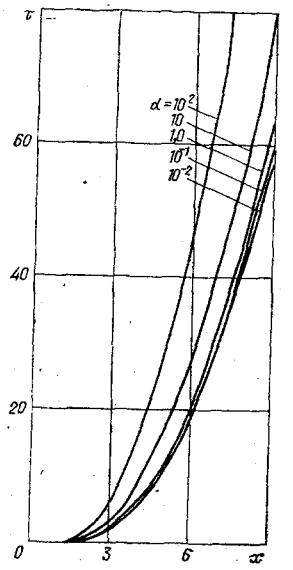

Fig. 2

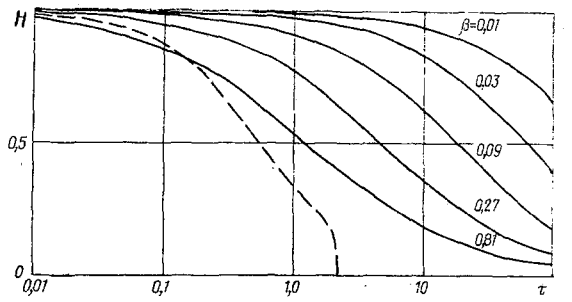

Fig. 3

types of solutions were expected in our problem. The calculation was therefore initially conducted over a small segment from the cavity boundary.

The computational region was doubled when the last computational value differed from the initial value by a magnitude on the order of 0.001%. Accuracy is thus increased to the required limit at the initial moment of time and it becomes possible to carry out the computation to any distance from the cavity.

Calculations were carried out in the study of the gas-pressure distribution and gas-filtration-rate distribution within a permeable medium within a wide range of variation of the dimensionless parameters: H_0 varied from 10^{-3} to 10^{-1}, α from 10^{-2}-10^2, β from 0.03 to 0.81; $\nu = 1$ and 3; $n = n_1 = 1$ (isothermal process).

Figures 1a and b depict the pressure distribution with respect to coordinate and time, respectively, in one form of the calculation: $\nu = 3$, $H_0 = 10^{-2}$, $\alpha = 1$, and $\beta = 0.03$. Dimensionless moments of time (Fig. 1a)

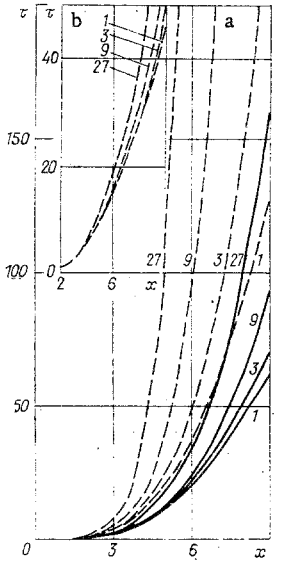

Fig. 4

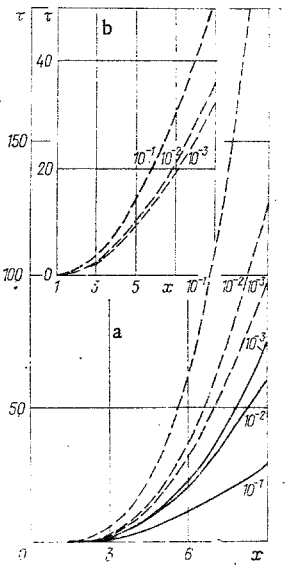

Fig. 5

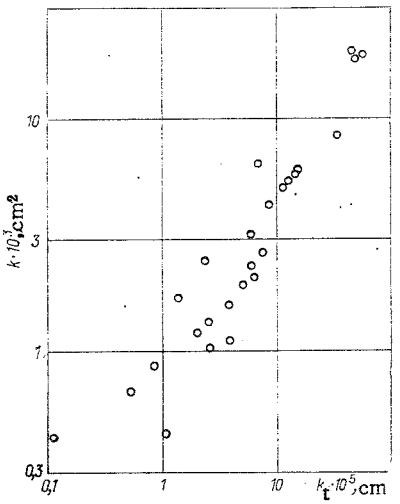

Fig. 6

TABLE 1

p_1, kg/cm² \ m, %	1	3	9	7
10	9,7	6,7	4,7	3,3
100	21,5	14,9	1 ,3	7,2

and coordinate x (Fig. 1b) are indicated on the curve by digits. The time at which the filtering gas arrives at different distances from the cavity, given these values of the dimensionless parameters ν, H_0, α, and β in the case of complete mixing of the cavity and interstitial gases in the disturbed region, was determined based on the computed gas-pressure distribution in the medium $H = f(x, \tau)$.

Since pressure at every point in space increases smoothly with time (Fig. 1b) and the moment at which it becomes difficult for pressure to increase was determined, the point at which the straight line, drawn correspondingly through the derivative maximum on the segment along which pressure increases, to the initial level of the interstitial pressure was plotted after the filtration "front" had arrived at a given distance.

TABLE 2

Group		ν	$\frac{W}{r_0}$	p_1, kg/cm²	r_0, m	Weakly fractured rock		Fractured rock		Strongly fractured rock, alluvium tufa	
	m, %					1		3		9	
	k, D					0,01	0,1	0,1	1	1	10
	k_T, cm					$4\cdot10^{-8}$	$8\cdot10^{-7}$	$8\cdot10^{-7}$	$1{,}4\cdot10^{-5}$	$1{,}4\cdot10^{-5}$	$3\cdot10^{-4}$
A	$\frac{t_s}{t_c}$	3	7,0	100	1	57 sec / 1,8 min	5,7 sec / 10,8 sec	18 sec / 48 sec			
					10	1,6 h / 3,0 h	9,6 min / 18 min	30 min / 1,3 h	3 min / 8 min	11 min / 1 h	
					20	6,4 h / 12 h	38 min / 1,2 h	2 h / 5,3 h	12 min / 32 min	44 min / 4 h	
					40	25,4 h / 48 h	2,5 h / 4,8 h	8 h / 21,3 h	48 min / 2,1 h	2,9 h / 16 h	17,6 min / 1,6 h
B	t_c	1	7,0	100	1	41 sec	4,1 sec	12,6 sec			
					10	1,1 h	7 min	21 min	2,1 min	7 min	
					20	4,6 h	28 min	1,4 h	8,4 min	27 min	2,7 min
					40	18,4 h	1,9 h	5,6 h	34 min	1,8 h	10,8 min
C	$\frac{t_s}{t_c}$	3	6,0	10	1	18,2 sec / 2 min	1,8 sec / 12,0 sec	1,3 min	7,7 sec		
					10	30 min / 3,3 h	3 min / 20 min	2,1 h	12,8 min		
				20	20	2 h / 13,2 h	12 min / 1,3 h	8,5 h	51 min		
					40	8 h / 58,2 h	48 min / 5,3 h	34 h	3,4 h		

Calculations were carried out for the arrival times of the cavity gas at different distances from the cavity in the simplest case when the cavity and interstitial gases did not mix. In this case the arrival time of the cavity gas to a fixed distance is characterized by the motion of the interface, which can be found from the equations

$$M_0 = \int_1^l 4\pi r^2 \rho dr \text{ when } \nu = 3; \quad M_0 = \int_1^l \pi r_0^2 \rho dr \text{ when } \nu = 1,$$

where M_0 is the mass of gas that has left the cavity, l is the interface coordinate, and πr_0^2 is the filtration channel area.

Thus the methods that have been used in this study to determine the arrival times of a filtering gas at a given distance yield, correspondingly, upper and lower bounds of this highly important characteristic of nonstationary filtration conditions.

Let us consider the influence of the dimensionless parameters on the gas-filtration process and determine the greatest actual values of α and β as the explosion products move through a disaggregated medium. The parameter α determines the nature of flow of the filtering gas. When $\alpha = 0$, flow is always laminar. In fact, if we pass in Eq. (8) to the limit $\alpha = 0$ and substitute the value of H in Eqs. (9) and (10), we obtain a problem corresponding to the Darcy law in the form

$$-\frac{\partial p}{\partial r} = \frac{\mu}{k} q \tag{16}$$

in place of Eq. (2). Therefore, we may use dependences obtained on the basis of Eq. (16) only when $\alpha \ll 1$ and it is necessary to use the two-term law (1) in separate cases.

This conclusion confirms, in particular, results of calculations of the position of the filtration front hodograph for values of α between 10^{-2} and 10^2, which are depicted in Fig. 2 (spherically symmetric gas

motion at a cavity pressure of 10^2 kg/cm^2 and medium porosity 1%) in one variant of the calculation when $\nu = 3$, $H_0 = 10^{-2}$, and $\beta_0 = 0.03$. It is evident that α does not strongly affect the motion of the filtration front in the range $0 < \alpha < 1$ and begins to substantially change the position of the front hodograph only when $\alpha > 1$.

We will use published data on the measurement of the permeability of rock that has been disaggregated by an explosion [6-8] in order to establish the greatest actual value of α. The zone of increased permeability is situated from 6-10 cavity radii from the explosion center depending on the type of rock and the natural state of the massif and also on explosion energy. Permeability in the zone of strong shattering varies from 10^{-1}-1 D and from 10^{-2}-10^{-1} D in the fracture zone. Such a range of variation of permeability leads to α being less than 1. In view of this fact and since the position of the filtration front hodograph in x and τ coordinates weakly depends on α when $\alpha < 1$, we assumed $\alpha = 1$ in the subsequent calculations.

It was also assumed that cavity cave in and the formation of a cave-in funnel occurs within time t significantly exceeding the characteristic filtration time, i.e., $t \gg m\mu r_0^2/p_1 k$. Therefore, the permeability of highly friable rock in a cave-in funnel, amounting to about 10-10^3 D, was not taken into account in this case.

The parameter β is directly proportional to medium porosity m and corresponds chiefly to the rate of pressure drop in the cavity. When $\beta = 0$, pressure in the cavity is constant. The influence of β on the nature of the variation of pressure in the cavity is depicted in Fig. 3 for $\nu = 3$, $\alpha = 1$, and $H_0 = 10^{-2}$. The dependence of cavity pressure on time determined for a 6.5-kg nuclear explosion at a depth of 240 m in alluvium with a density of 1.9 g/cm^3 and moisture of 12% [9] is depicted by the broken curve. The free porosity is about 15% for an alluvium porosity of 25-30% and moisture of 12%, which corresponds to $\beta \sim 0.45$. The broken line is situated between the curves for $\beta = 0.27$ and $\beta = 0.81$ for low τ, though the measured pressure subsequently decreases more strongly than the computed pressure. This difference is explained by the obvious fact that thermal processes in the calculation were not taken into account.

Figures 4a and b depict the influence of porosity m on arrival time of the filtration front (unbroken curves) when $\nu = 3$ and when the interface moves (broken curves) for $\nu = 3$ and $\nu = 1$. In all cases, $\alpha = 1$ and $H_0 = 10^{-2}$. The value of m is indicated in percent on the curves.

The influence of gas pressure in the cavity on the speed of the filtration front (unbroken curves) is illustrated by Figs. 5a and b for $\nu = 3$ and $\nu = 1$, respectively. The broken curves depict the position of the interface. Values of H_0 are indicated on the curves. In all the cases, $\alpha = 1$ and $m = 0.01$. The interface moves less rapidly in the case of equal cavity pressure when $\nu = 3$ than when $\nu = 1$.

The calculated dependence of filtration-front arrival time on distance in the absence of cavity cave in in the case $\alpha = 1$, $p_1 = 10^2$ kg/cm^2, and $m = 0.01$ can be described by interpolation formulas in the spherically symmetric case ($\nu = 3$, $\beta = 0.03$) $\tau = 0.1122\, x^{3.22}$ where $3.0 < x < 10$, while in the two-dimensional case ($\nu = 1$, $\beta = 0.0075$)

$$\tau = 0.692\, x^{1.9},\ 2.0 < x \leqslant 10.$$

Gas flow through a fixed surface in the case $\nu = 1$, $\alpha = 1$, $\beta = 0.0075$, and $H_0 = 10^{-2}$ when $\tau > 0.3$ can be represented in the range $2 < x < 10$ in the form

$$Q = \frac{0.423}{\tau^{0.51}} - \frac{0.177}{\tau^{1.61}}[x - 0.06\exp(0.1135\tau)]^3,\ x > 0.06\, e^{0.1135\tau};$$

$$Q = \frac{0.423}{\tau^{0.51}},\ x \leqslant 0.06\exp(0.1135\tau).$$

The calculation demonstrated that there exists a limiting distance $L_m = W_m/r_0$ to which the interface between the explosion products and air propagates in the absence of mixing, depending on the porosity of the medium and gas mass in the cavity. This distance can be expressed in terms of m and cavity pressure H_0,

$$\frac{W_m}{r_0} = \left[\frac{1 - H_0(1-m)}{H_0 m}\right]^{1/3} \text{ when } \nu = 3;$$

$$\frac{W_m}{r_0} = \frac{4[1 - H_0(1 - 0.75m)]}{3H_0 m} \text{ when } \nu = 1.$$

Table 1 presents values of the limiting distances L_m when $\nu = 3$ for a number of values of m and p_1.

The time at which the cavity gas is discharged into the atmosphere is in practice the most important characteristic of an underground explosion. Since in carrying out the calculations we have assumed that the medium was infinite, the moment of arrival of the filtration front or of the interface to a hypothetical free surface situated at a required distance W from the point of explosion was taken as the time at which the gas is discharged into the atmosphere.

The time t_s at which the filtration front discharged into the atmosphere and the time t_c at which the interface is likewise discharged are presented in Table 2 for a number of rocks characterized by differing degrees of fracturing, porosity, and permeability k and k_t for a typical depth of the camouflaged explosion W between $6r_0$ and $7r_0$. Times in the case of a spherically symmetric ($\nu = 3$) motion can be found in the group of rows indicated by A (Table 2) and times in the case of two-dimensional ($\nu = 1$) motion when $p_1 =$ 100 kg/cm^2 and distance to the free surface $W = 7r_0$ are given in the group of rows indicated by B. The C group of rows contains arrival times when $\nu = 3$, $p_1 = 16$ kg/cm^2, and $W = 6r_0$.

Values of the turbulent permeability coefficient k_t are taken from an empirical dependence between k and k_t (Fig. 6) constructed using previous [2] data. The value of μ was taken equal to $2 \cdot 10^{-4}$ p, which corresponds to the viscosity of carbon dioxide at a temperature of about 40°C and pressure of about 60 kg/cm^2. The scale of the explosion is determined by the cavity radius r_0. It is clear from Table 2 that the time at which the explosion products are discharged into the atmosphere substantially depends on the filtration characteristics of the disaggregated medium and the explosion scale. Thus, discharge time strongly decreases as medium porosity and permeability increase. The influence of explosion scale on discharge time is particularly great. A 200-400% increase in the linear explosion scale increases the discharge time of the cavity gas by more than 500-1000%.

We note that the disaggregation region is usually prolate upwards in a camouflaged explosion due to the presence of break-away disaggregations and the freedom with which the medium shifts towards the crestal plane. It therefore seems that the initially organized spherically symmetric gas motion assumes the nature of two-dimensional motion at the last stage. We may therefore suppose that the actual times at which the gas is discharged into the atmosphere will have intermediate values between that calculated for $\nu = 3$ and $\nu = 1$. Moreover, a cave-in column will form in great explosions when the cavity roof is insufficiently stable over time $t < m\mu r_0^2/p_1 k$ and the data in Table 2 may turn out to be overstated.

The inertial terms $\rho(\partial u/\partial t)$ and $\rho u(\partial u/\partial r)$ were eliminated from the motion equation in solving the problem. An estimate of the inertial terms after the calculations were carried out, shows that they are quite negligible, since they are two to three orders of magnitude less than the remaining terms of the motion equation.

These results of the calculations can be improved if we begin to consider thermal processes, take into account the dependence of porosity on distance from the explosion point and gas viscosity on temperature, and also refine the pressure of the explosion gases in the cavity as a function of the type of explosion source, soil characteristics, and explosion scale.

LITERATURE CITED

1. L. S. Leibenzon, Motion of Natural Fluids and Gases in a Porous Medium [in Russian], Gostekhizdat, Moscow (1947).
2. G. F. Trebin, Filtration of Fluids and Gases in Porous Media [in Russian], Gostoptekhizdat, Moscow (1959).
3. A. E. Scheidegger, Physics of Flow through Porous Media, University of Toronto Press (1960).
4. V. V. Adushkin and L. M. Pernik, "Distinctive features of the formation of funnels of collapse," Fiz. Goreniya Vzryva, 8, No. 4 (1972).
5. G. I. Marchuk, Methods of Computational Mathematics [in Russian], Nauka, Novosibirsk (1973).
6. S. Derlich, "Environmental change due to an underground nuclear explosion," in: Peaceful Nuclear Explosions, Vienna (1970), pp. 123-138.
7. C.R. Boardman, "Engineering effects of underground nuclear explosions," in: Proceedings of a Symposium on Engineering and Explosions, Las Vegas, Nevada, 1970, Vol. 1, Springfield, Virginia (1970), pp. 43-67.
8. C. W. Olsen, "Time history of the cavity pressure and temperature following a nuclear detonation in alluvium," J. Geophys. Res., 72, No. 20 (1967).